https://doi.org/10.1590/jatm.v18.1448

ORIGINAL PAPER

Aerodynamic Performance of Rectangular Counter-Rotating Vortex Generators on Amphibious Plane Airfoils

Gunawan Wijiatmoko[1,2,*], Eflita Yohana[1], Mohammad Tauviqirrahman[1], Bobby Ezra Maulana[1], Shofwan Bahar[1], Ivransa Zuhdi Pane[2]

1. Diponegoro University – Faculty of Engineering – Department of Mechanical Engineering – Semarang – Indonesia. .
2. National Research and Innovation Agency Research – Center for Aeronautics Technology – South Tangerang – Indonesia.

*Corresponding author: guna001@brin.go.id

ABSTRACT

Inter-regional connectivity is a crucial necessity in various emergencies; however, the limited standard of runways in remote areas poses operational challenges for conventional aircraft. This study aims to investigate the influence of geometric parameters and installation positions of rectangular counter-rotating vortex generators (VGs) on a NACA 4415 airfoil used for short take-off and landing (STOL) amphibious planes. Numerical simulations using the Reynolds-averaged Navier-Stokes k-ω shear stress transport turbulence model were conducted to analyze aerodynamic performance across various angles of attack. The results indicate that VGs effectively delay flow separation and improve the lift-to-drag ratio, particularly at medium to high angles of attack. Geometric parameters such as a height of 30 mm and a length of 4.5 *h* proved to provide the most rational performance for take-off and landing conditions. However, the installation of VGs also introduces adverse effects in the form of increased parasitic drag at low angles of attack, potentially impacting fuel consumption during the cruise phase. Overall, the proper configuration of VGs significantly enhances the safety and operational efficiency of amphibious aircraft on short runways.

Keywords: Vortex generators; Amphibious aircraft; Aerodynamic characteristics; Flow separation; Computational fluid dynamics; STOL aircraft.

INTRODUCTION

The aircraft industry has made a breakthrough in the world of transportation. The aviation industry offers connectivity between cities and islands, which is critical in health emergencies, natural disasters, and fires (Große *et al.* 2021). Air transportation is very relevant for reaching remote areas, mainly when the area is limited by waters that separate one region from another, so land or sea transportation is not the right choice regarding cost and time efficiency (Karyawan *et al.* 2024). Airplanes are one of the promising modes of transportation, and their use can significantly help connectivity and tourism between regions (Mazzola *et al.* 2022), but the construction of runways and airports in remote areas is a challenge for local area managers and it's often, runways in remote areas are not up to standard, making it difficult to operate an aircraft in the region, which is why the ability of the aircraft to take off and land over short distances is essential (Meyer *et al.* 2021).

Received: Oct. 04, 2025 | **Accepted:** May 07, 2026
Peer Review History: Single Blind Peer Review.
Section editor: Paulo Greco

Boundary layers affect both lift and drag forces in fluid mechanics, making the improved control of boundary layers a vital focus of research (Algan *et al.* 2024; Nath *et al.* 2021). This phenomenon has an impact on the performance of various technical applications involving fluid flow, such as in the automotive, aerospace, and energy generation fields (Ichikawa *et al.* 2021; Li *et al.* 2024; Utomo *et al.* 2024). Flow control techniques can be categorized into active and passive. The active approach necessitates external energy for its implementation, whereas the passive methods operate without the need for external energy to regulate the flow (Algan *et al.* 2024). Flow separation control by utilizing passive devices is currently the cheapest and fastest solution to implement. The addition of vortex generators (VGs) on aircraft wings is one way to help aircraft improve aerodynamic take-off and landing capabilities (Szabó *et al.* 2024; Tsipenko *et al.* 2022). A VG is a device employed to regulate boundary layer phenomena and mitigate the possibility of airflow separation around an aircraft's wings. The vortex caused by VGs drives momentum transfer from the high-velocity region to the low-velocity region near the wall (boundary layer) (Chung *et al.* 2023). This phenomenon reduces the boundary layer's depth, delays and suppresses separation of the flow, which will indirectly increase the lifting capacity.

Several investigations have been conducted to assess the impact of VG interaction on aerodynamic performance. Algan *et al.* (2024) performed an experimental study on the NACA 4415 airfoil at a Reynolds number of 1.4×10^5, demonstrating that the inclusion of VG resulted in a 107.7% increase in the lift coefficient (C_L), a 23.39% reduction in drag coefficient (C_D), and a delay in stall by 4° relative to its reference performance. There is also research conducted by Chen (2021), who added a VG to the Bell A821201 type airfoil at a Reynolds number of 4.5×10^6, revealing a significant improvement in aerodynamic characteristics. The C_L exhibited a 62.23% increase, accompanied by a 10° extension of the stall angle. Additionally, the C_D of the airfoil using vortex-producing components was reduced by 53.37%. Research on VGs installed on FFA-W3-301 and FFA-W3-360 airfoils was also carried out by Li *et al.* (2019) using both numerical and experimental methods. Findings from this study indicated that VG increased the stall angle by 10°, increased the C_L by 48.7%, and reduced C_D by 84.9% at the maximum angle.

The effectiveness of VG depends on its geometry and orientation, which are regulated based on specific operational circumstances. Geometric parameters of VGs significantly affect the aerodynamic behavior acting on an aircraft wing. These geometric and installation characteristics are largely determined by the depth of the boundary layer that develops over the wing's surfaces. Vortex generators can be engineered in various forms and tailored to meet specific aerodynamic needs. The efficacy of VGs has been the subject of numerous studies that have investigated the impact of geometric parameters. Experimental research by Manolesos *et al.* (2023) regarding the conventional size of the vortex of a square-shaped generator, it was found that the conventional VG size produces a vorticity that is too strong, causing additional resistance compared to the smaller VG. Manolesos *et al.* (2023) also conducted research related to the placement of VG and concluded that the quantity of vortices produced is directly proportional to the increase in the angle of incidence of the VG. Numerical research by Zhen *et al.* (2011) and experimental research by Chung *et al.* (2023) regarding the influence of the VG position on aerodynamic performance state that the effective position of the VG moves further forward in accordance with the angle created between the airfoil and the relative wind. A study conducted by Verma and Sankar (2024) about the significance of the distance between each vane and its effect on the effectiveness of the vortex force produced by VG it is asserted that reducing the distance between vanes in the VG will create more controlled airflow in the separation region.

Research on the aerodynamic characteristics of VGs is often conducted using experimental (Hao *et al.* 2023) and numerical methods. (Zhu *et al.* 2021). Experimental methods are considered expensive and time-consuming for developing an initial design to find the optimal design (Rokhman *et al.* 2024). Today, numerical techniques have become an integral aspect of analysis. In particular, computational fluid dynamics (CFD) simulations allow for a thorough evaluation of the characteristics of the flow field and can better explain physical processes. (Khaled and Aly 2022).

Studying the influence of geometry and installing VGs is an important and challenging task because amphibious aircraft require efficiency and great lift to be able to take off or land in a short time over short distances.

This investigation intends to analyze geometric and installation parameters such as height, length, vane distance, position, and yaw angle of counter-rotating VG in a short take-off and landing (STOL) type amphibious passenger aircraft at the minimum speed during take-off or landing.

METHODOLOGY

Governing equation

Computational Fluid Dynamics (CFD) is a numerical simulation method (in this study, carried out using the ANSYS Fluent 2023 R2 software) based on the governing equations of fluid mechanics, namely the continuity and Navier-Stokes equations. For the turbulent flow conditions investigated in this study, the Reynolds-averaged Navier-Stokes equations are employed (Tleubergenova *et al.* 2023; van Druenen and Blocken 2023). These equations are solved using the k-ω shear stress transport (SST) turbulence model, which is well-suited for predicting flow separation and adverse pressure gradients on aerodynamic surfaces.

The basic equations for computational control are the continuity equation of (mass conservation), which asserts that the rate of change within a fluid element corresponds to the rate of mass flow into the element, as written in Eq. 1, and the momentum equation (Newton's second law), which is expressed in Eq. 2 below (Sulistiya and Kasman 2019):

$$\frac{\partial \rho}{\partial t} + \frac{\partial \bar{u}_i}{\partial x_i} = 0 \tag{1}$$

$$\frac{\partial}{\partial t}(\rho\, \bar{u}_i) + \frac{\partial}{\partial x_j}\left(\overline{\rho\, u_i'\, u_j'}\right) = -\frac{\partial \bar{P}}{\partial x_i} + \frac{\partial}{\partial x_j}\left(\mu\left(\frac{\partial \bar{u}_i}{\partial x_j} + \frac{\partial \bar{u}_j}{\partial x_i}\right) - \left(\overline{\rho\, u_i'\, u_j'}\right)\right) + g_i \tag{2}$$

where x_i and x_j are the coordinates, $\bar{u}_i$ and $\bar{u}_j$ represent the averages of the speed components, $\bar{P}$ is the average pressure, ρ is the density, g_i is the acceleration of the gravity axis of inertial coordinates, μ is the effective viscosity coefficient of dynamic viscosity, and $\overline{\rho\, u_i'\, u_j'}$ is the Reynolds stress.

In this study, the SST k - ω turbulence model was used because it has the ability to represent the phenomenon of fluid flow near the wall well (Yan *et al.* 2019; Wang *et al.* 2023). This turbulence model is widely used by other researchers in phenomena related to aerodynamic problems, not only in the flow of fluid around the airfoil (Sulistiya and Kasman 2019; van Druenen and Blocken 2023; Yan *et al.* 2019), but also on various other objects (Bao *et al.* 2020; Li *et al.* 2023). The equations of the SST model are written in Eqs. 3 and 4 (Sulistiya and Kasman 2019):

$$\frac{\partial}{\partial t}(\rho\, k) + \frac{\partial}{\partial x_j}(\rho\, k\, u_i) = \frac{\partial}{\partial x_j}\left(\Gamma_k \frac{\partial k}{\partial x_j}\right) + G_k - Y_k + S_k \tag{3}$$

$$\frac{\partial}{\partial t}(\rho\, \omega) + \frac{\partial}{\partial x_j}(\rho\, \omega\, u_i) = \frac{\partial}{\partial x_j}\left(\Gamma_\omega \frac{\partial \omega}{\partial x_j}\right) + G_\omega - Y_\omega + S_\omega \tag{4}$$

where G_0 represents generated turbulence kinetic energy, Γ is the effective diffusivity, and Y_k is the rate of successive turbulence dissipation for k and ω.

The pressure-velocity coupling was handled using the semi-implicit method for pressure-linked equations algorithm. To ensure high spatial accuracy, a second order of approximation was used to discretize the governing equations. Specifically, second-order schemes were applied to the pressure and momentum terms to minimize numerical diffusion. For the convective terms, appropriate schemes were utilized to balance higher-order accuracy with the stability required for a robust computational iterative process (Wijiatmoko *et al.* 2024).

To ensure a well-defined numerical problem, the following boundary conditions were applied to the computational domain: the inlet was defined as a velocity inlet condition, set with a uniform flow velocity of 30 m/s, corresponding to the aircraft's minimum take-off speed. The turbulence intensity was set to 5%, and the turbulent viscosity ratio was 10. The outlet was defined as a pressure outlet condition, which was applied with a static gauge pressure of 0 Pa (ambient atmospheric pressure). The VG surfaces were assigned a no-slip wall condition assigned to the surfaces of the NACA 4415 airfoil and the rectangular VGs. As a fluid domain wall, these were set as slip walls (depending on the specific mesh setup) to simulate unconfined flow and reduce boundary interference.

Geometry model

The simulation was conducted on an airfoil corresponding to the mean aerodynamic chord of an amphibious aircraft. For more details, Table 1 and Fig. 1 show the primary geometry parameters used in the numerical simulation.

Table 1. Airfoil and VG geometry.

Dimension	Symbol	Value
Airfoil type	-	NACA 4415
Chord length	L	2,100 mm
Spanwise length	S	1,000 mm
VG pair distance	p	0.1 L
VG height	h	20 mm; 30 mm; 40 mm
VG length	l	3 h; 4.5 h; 6 h
VG distance	d	0.8 h; 1.2 h; 1.6 h
Position	X	0.1 L; 0.125 L; 0.15 L
VG angle of incidence	β	10°; 14°; 18°
Angle of attack	α	0°–18°

Source: Elaborated by the authors.

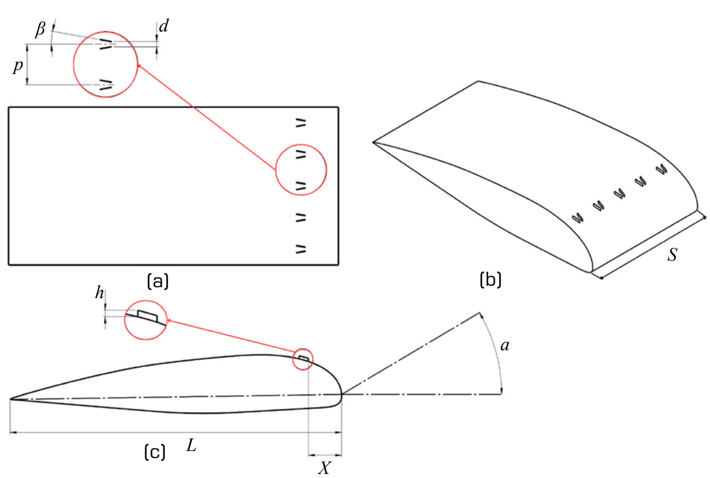

Source: Elaborated by the authors.

Figure 1. Schematic and nomenclature of airfoil amphibious aircraft and VG. (a) Top; (b) Isometric; (c) Side.

Fluid domain

In external flow simulations, particularly for airflow around wing surfaces, the fluid domain must be carefully defined. This allows the accurate representation of how the wing influences the surrounding airflow, while ensuring that the computational demands remain within practical capabilities (Wijiatmoko *et al.* 2024). The domain size, as shown in Fig. 2, was used in this study to avoid the effect of fluid domain walls that can interfere with the flow. (Golmirzaee and Wood 2024).

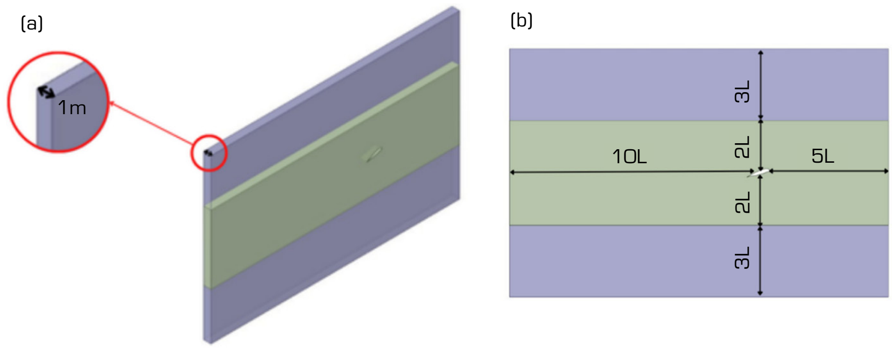

Source: Elaborated by the authors.

Figure 2. Fluid domain. (a) Isometric view; (b) Side view.

Mesh generation

The body of influence in the study aims to capture the flow phenomenon around the airfoil and VG. The boundary layer phenomenon was also studied using the inflation generation feature near the airfoil wall and the VG to capture the boundary layer event in regions very close to the airfoil wall of the amphibious aircraft wing. Details of the formation of elements in the simulation can be seen in Fig. 3. It can be seen that the mesh arrangement is made dense around the airfoil and densified around the VG to capture the effect of the resulting vorticity.

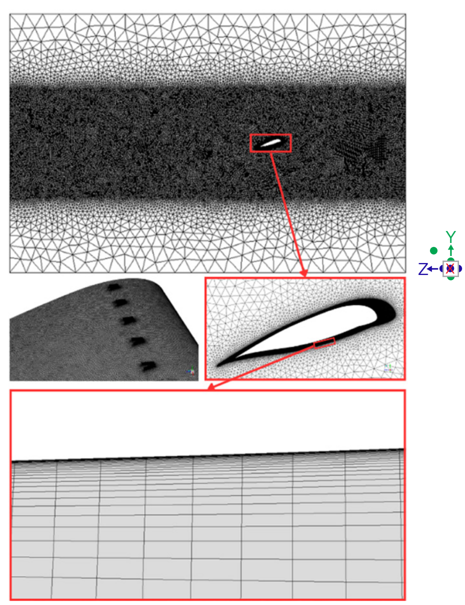

Source: Elaborated by the authors.

Figure 3. Details of mesh generation.

In addition to size, the quality of the mesh also needs to be considered. The quality of this mesh can be reviewed based on the skewness value, orthogonal quality, and y^+. Skewness indicates the asymmetry of grid elements, whereas orthogonal quality measures the regularity of angles between grid elements. At the same time, y^+ indicates the mesh quality for representing near-wall phenomena by estimating the distance from the wall surface to the first grid node.

The estimation *of* y^+ can be performed utilizing the following Eq. 5. (ITTC 2011):

$$\frac{y}{L} = \frac{y^+}{\left(Re\sqrt{\frac{Cf}{2}}\right)} \quad (5)$$

Based on the mesh quality shown in Table 2, the skewness and orthogonal quality values are in the acceptable category. Based on the results of previous studies, the quality of the formation of mesh elements in the case of separation flows near the surface of the airfoil must be maintained at a value of $y^+ < 5$. (Fouatih *et al.* 2019). Figure 4 shows the contour of the y^+ value on the geometric wall.

Table 2. Quality of element generation.

Mesh parameters	Value
Skewness maximum	0.841
Orthogonal minimum	0.159

Source: Elaborated by the authors.

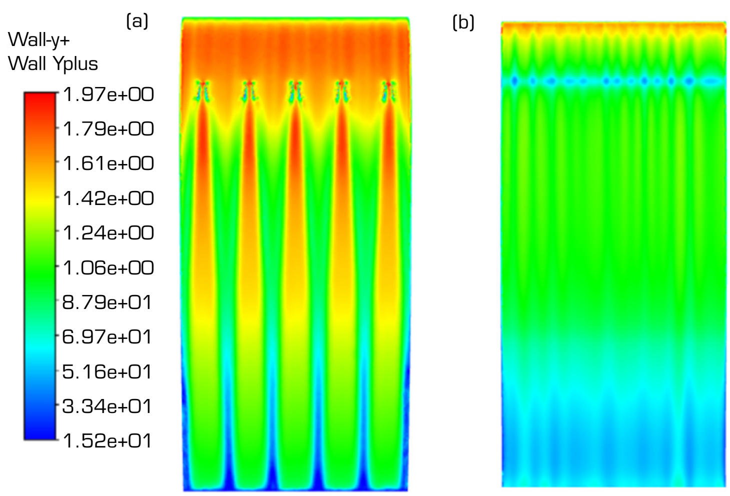

Source: Elaborated by the authors.

Figure 4. Y^+ contour around the geometry. (a) Top view; (b) Bottom view.

The grid independence test in Fig. 5 was performed by comparing one of the output parameters against the number of mesh elements. The allowed error in grid independence tests should be less than 5%. (Aliffrananda *et al.* 2022). The results of the grid test process show that the number of elements used is optimal and does not significantly affect the results of the simulation performed. The smallest error value was 0.16%, with a total of 6.6×10^6 elements. However, in this study, 6.35×10^6 elements were used because the error value was still less than 1%, while using a smaller number of elements, so the computing time could be shorter than if 6.6×10^6 elements were used.

Validation study

For validation, this study compared C_L and C_D with the results from Fouatih's (2016) experimental research, which investigated the effect of adding a VG to the NACA 4415 airfoil at $Re = 2 \times 10^5$. Figure 6 presents the comparison between the simulation and the journal's results at four distinct angles. The variation between the two results remained under 5% in all cases, with an average error of 2.80%. This result is well below the maximum threshold of validation margin error, which is 10% (Duan *et al.* 2019; Seth and Liem 2021).

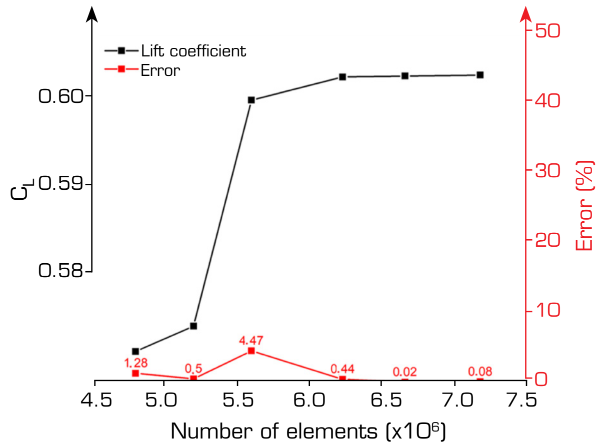

Source: Elaborated by the authors.

Figure 5. Grid independence test.

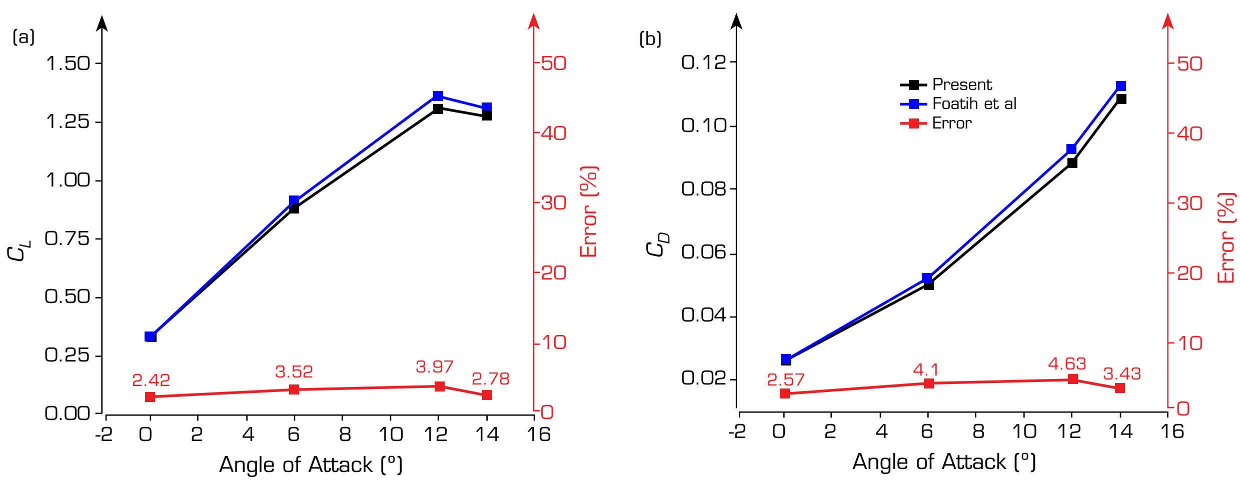

Source: Elaborated by the authors.

Figure 6. Validation study based on: (a) C_L; (b) C_D.

RESULTS AND DISCUSSION

Baseline performance

The performance of an aircraft is contingent upon various factors, among which the geometry of the airfoil is an essential element in determining its aerodynamic efficiency. This stage aims to understand the characteristics and performance of the amphibious aircraft airfoils used. The test was carried out at the minimum speed of the aircraft during the take-off phase, which was 30 m/s. The data presented represent the aircraft's performance at Re = 4.3×10^6, as shown in Fig. 7, in the form of C_L, C_D, and lift-to-drag ratio (*L/D*). Baseline data are needed to specify the critical angle of attack of the amphibious airfoil, as well as comparative data for aerodynamic performance before and after using the VG.

The graph in Fig.7 shows that the C_L will decrease after reaching the maximum angle of attack. The highest C_L was observed at ($\alpha = 16°$), which shows that this airfoil has a critical angle of attack at ($\alpha = 16°$) with a C_{Lmax} of 2.18 and a C_D of 0.34. The *L/D* provides a measure of the airfoil's efficiency. The ratio has increased starting from ($\alpha = 0°$), reaching its peak value at ($\alpha = 4°$), and decreases as the angle continues to rise. At the critical angle of attack, this airfoil has an *L/D* ratio of 6.52.

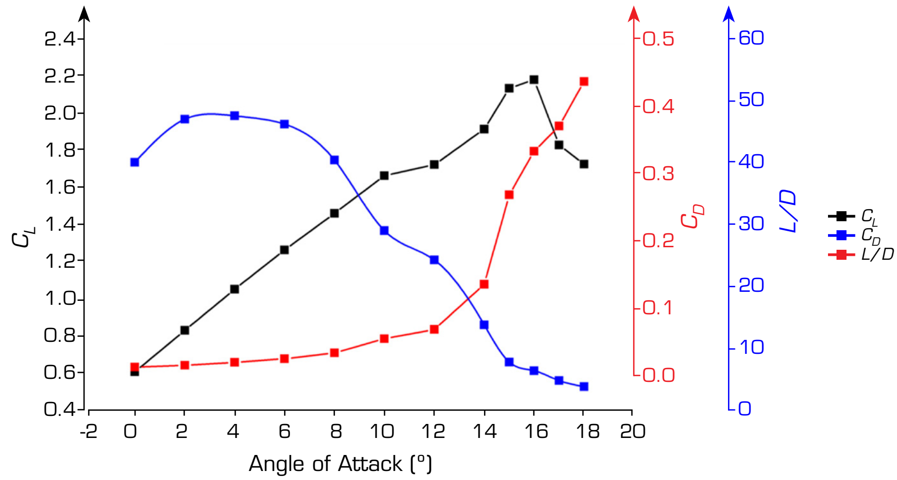

Source: Elaborated by the authors.

Figure 7. Baseline performances.

Influence of geometric parameters

The geometric aspect greatly influences the vortex power generated from the VG. The geometry of the VG, such as its height and length, plays a crucial role in creating a stable and effective vortex for controlling airflow. Vortex generators (VGs) with optimal geometry can reduce drag and improve climbing and descending efficiency in aircraft. (Meyer *et al.* 2021).

Effect of VG height

The height of VGs affects the amount of vortex force created and has an impact on aerodynamic performance. Each angle of attack has a different size of boundary layer, so it is essential to comprehend the effect of the VG height at various angles. Three height variations of the VG were simulated, namely 20 mm, 30 mm, and 40 mm, with a length of 3 h; the distance between VGs was 1.2 h, positioned at 0.15L from the leading edge, and the angle of incidence was 10°. Figure 8a-c shows the C_L, C_D, and L/D, respectively.

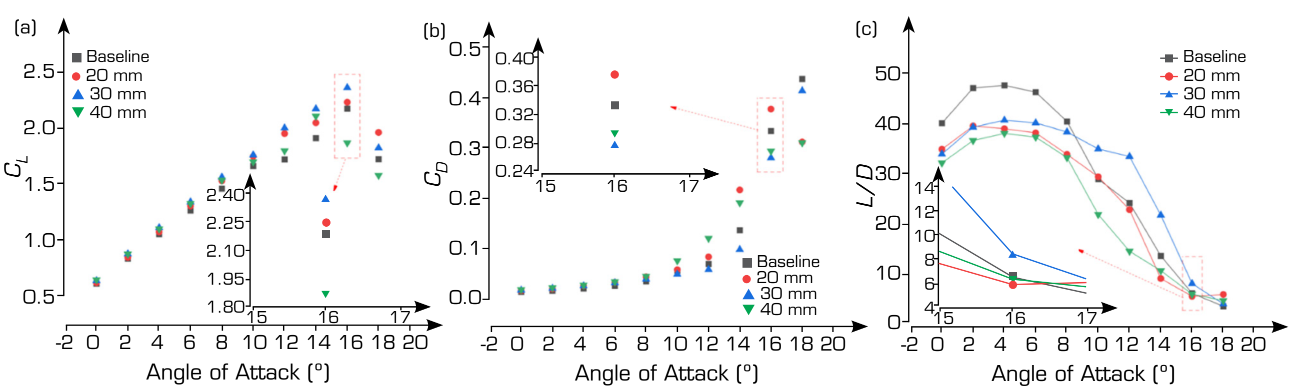

Source: Elaborated by the authors.

Figure 8. The effect of VG's height on: (a) C_L; (b) C_D; (c) L/D.

The effect of the VG's height on lifting capabilities at multiple angles is shown in Fig. 8a. At the angle of attack (0° ≤ α ≤ 14°), each variation in the height of the VG has a higher C_L compared to the previous one. The difference occurred at the critical angle of attack, where the high variations of 20 mm and 30 mm gave an increase in the C_{Lmax} of 2.61% and 8.61%, respectively, while the variation of 40 mm experienced a decrease in the C_{Lmax} value of -14.11% compared to the baseline C_L before using the VG.

Same phenomenon of declining performance was also observed by Yan *et al.* (2019). As illustrated in Fig. 8a and b, an increase in the VG height leads to a greater concentration of vorticity and stronger flow control, but it could also lead to greater resistance. (Li *et al.* 2019).

The effectiveness of aerodynamic performance can be seen through the ratio between the C_L shown in Fig. 8a and the C_D in Fig. 8b. Figure 8c shows that at the angle of attack ($0° \leq \alpha \leq 8°$), the entire addition of the VG has a negative impact on the *L/D* ratio. This happens because the fluid flow tends to be still bound to the surface around the airfoil, so the resulting vortex damages the flow around the wing and results in a decrease in the effectiveness of aerodynamic performance. However, it can be seen that at the angle of attack($0° \leq \alpha \leq 2°$), the VG with a height of 20 mm has a higher *L/D* ratio compared to the other variations. However, when at the angle of attack ($4° \leq \alpha \leq 16°$), the height variation of 30 mm has the highest effectiveness among the other three variations. These results indicate that a VG with low height is more effective at small angles of attack and vice versa (Hares *et al.* 2019). The phenomenon of adding a VG occurs in the geometry with a height of 30 mm at the angle of attack ($10° \leq \alpha \leq 16°$), which provides an increase in the *L/D* ratio of 20.42%–57.94% compared to the initial performance.

Figure 9 shows the contour of turbulence intensity around the airfoil of the amphibious aircraft wing, especially at the rear of the airfoil, where the red contour characterizes the flow with high turbulent intensity. Based on the level of turbulence intensity, the addition of a VG with a height of 30 mm at an angle of 16° can reduce the turbulence intensity that occurs and produce the lowest turbulence when compared to the other variations. This is because the VG can transfer sufficient energy into the boundary layer while causing only a modest increase in drag (Yan *et al.* 2019).

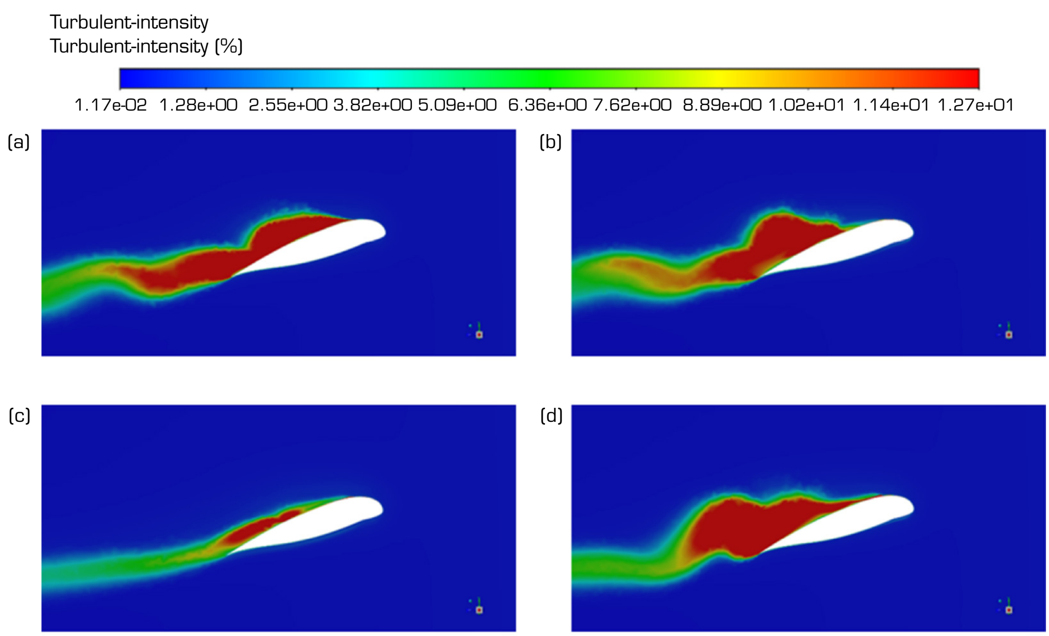

Source: Elaborated by the authors.

Figure 9. Contour of the effect of the height of the VG on the turbulence intensity. (a) Baseline; (b) 20 mm; (c) 30 mm; (d) 40 mm.

Effect of VG length

Vortex's strength is also influenced by the VG's length. The number of vortices needed to enhance fluid flow around the wing changes with the increase in angle of attack. Three VG variations were simulated to investigate the influence of length on aerodynamic efficiency and capabilities, namely 3 *h*, 4.5 *h*, and 6 *h*, with a height of 20 mm, the distance between VGs was 1.2 *h*, the VG position was at 0.15 *L*, and the angle of incidence was 10°. The illustration of VG length on aerodynamic performance is presented in Fig.10a-c.

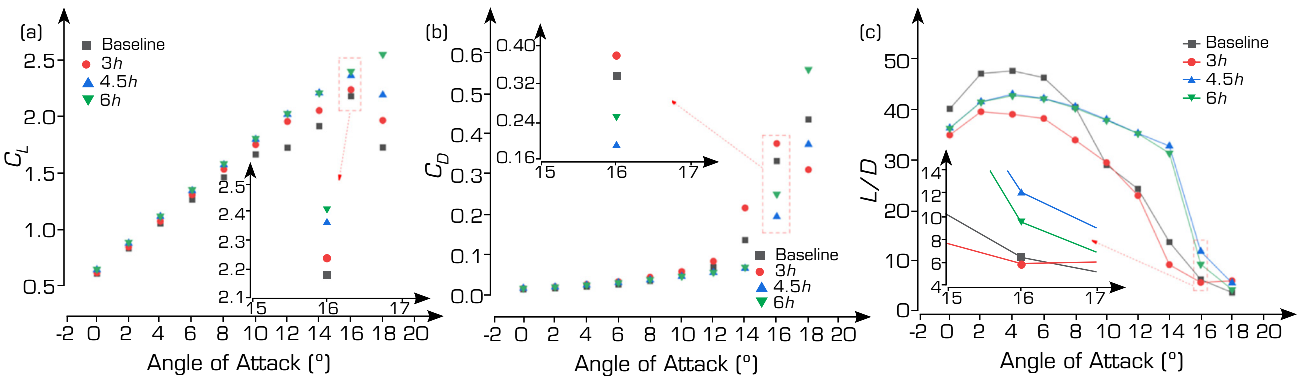

Source: Elaborated by the authors.

Figure 10. Effect of *VG* length on: (a) C_L; (b) C_D; (c) *L/D*.

The C_L and C_D values shown in Fig. 10a and b will affect the effectiveness of aerodynamic performance. According to the simulation, the performance effectiveness shown in Fig. 10c shows that the implementation did not give a positive impact when the wing was at (0° ≤ α ≤ 8°), but at (8° ≤ α ≤ 16°), the VG with a length variation of 4.5 *h* had the highest performance effectiveness value compared to the other two length variations. The 4.5 *h* vortex length of the generator at the angle (8° ≤ α ≤ 16°) provided an increase in the *L/D* ratio of 0.15%–136.02% compared to the benchmark performance. The 6 *h* length variation ranked second and was followed by the 3 *h* length variation as the variation with the lowest level of effectiveness. A similar phenomenon was also found by Hares *et al.* (2019) in their research related to the influence of VG length. This result was obtained because the VG with a length of 3 *h* produced a vortex that was less able to transfer energy to the low-energy airflow behind the airfoil and resulted in a turbulence intensity that was not significantly reduced, while the 4.5 *h* variation created the most optimal vortex strength to control flow separation, so that there was not much high-intensity turbulent flow around the aircraft wing. Although the VG with a height of 6 *h* was able to control the flow separation around the wings, the resulting vorticity was too large, making it ineffective and producing unnecessary drag. Although the angle (8° ≤ α ≤ 16°) height of 6 *h* did not give the best results, the variation succeeded in inhibiting the separation phenomenon that occurred at the angle of attack (α > 16°) and delayed the stall that occurred at an angle of 16°. Figure 11 represents a comparison of turbulence intensity in each variation, which supports the previous explanation.

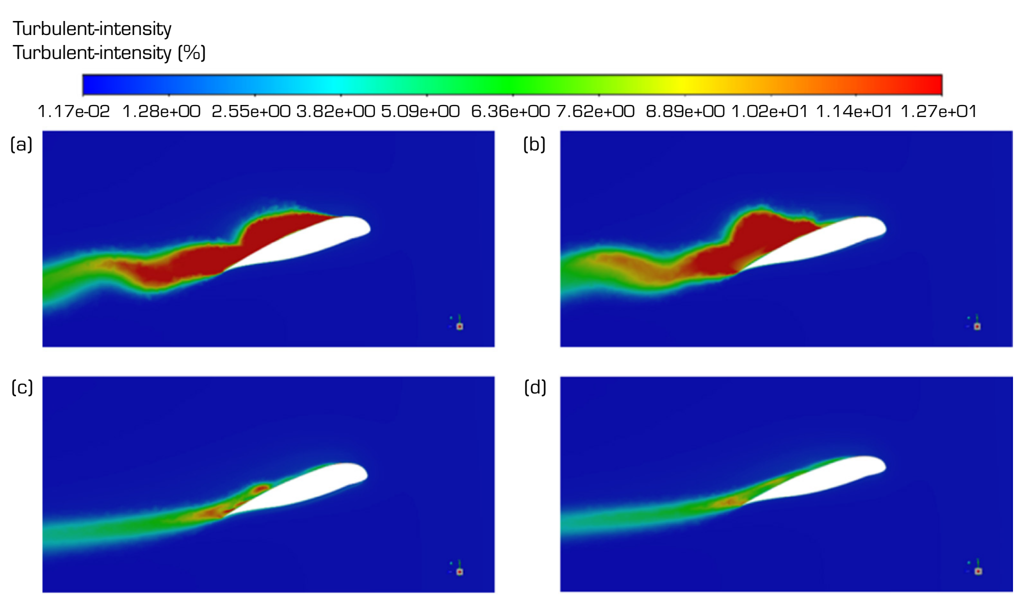

Source: Elaborated by the authors.

Figure 11. Contour of the effect of VG length on turbulence intensity. (a) Baseline; (b) 3 *h*; (c) 4.5 *h*; (d) 6 *h*.

Influence of installation parameters

In addition, the installation parameters of the VG are also crucial. The installation location and orientation determine the interaction between the generated vortices and the surrounding airflow. An optimally placed VG can improve airflow control and delay flow separation, ultimately improving overall stability and performance.

Effect of vane distance

Three variations of the VG were simulated to examine the distance effect between vanes on aircraft performance, ranging from 0.8 *h*, 1.2 *h*, and 1.6 *h*, with a 20 mm height, a length of 3 *h*, the position of the VG against the leading edge at 0.15 *L*, and the angle of incidence set at 10°. The influence of VG distance on aerodynamic efficacy is presented in Fig. 12a-c.

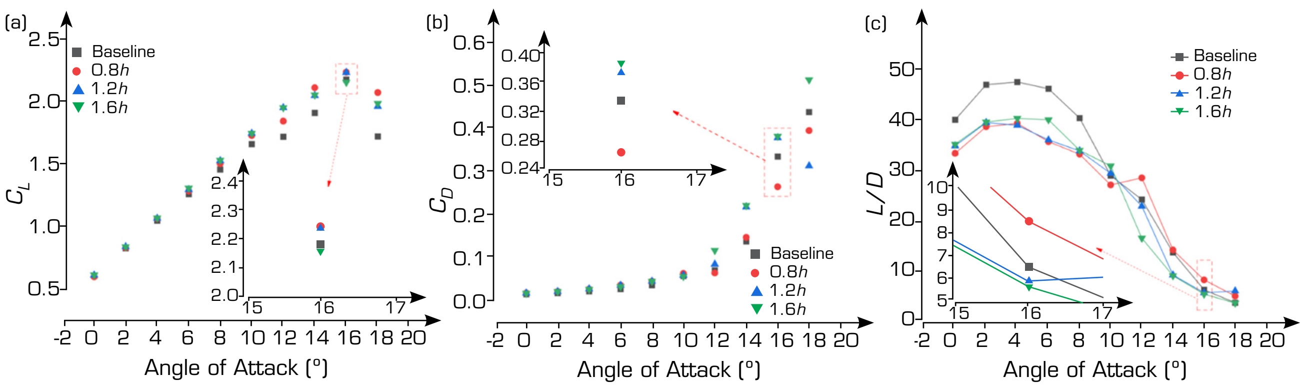

Source: Elaborated by the authors.

Figure 12. Effect of distance between vane on: (a) C_L; (b) C_D; (c) *L/D*.

The distance between the VGs affects the ability to control the separation flow (Li *et al.* 2019), where the optimal distance between the VGs varies at each angle of attack. An increased range on the VG results in improved performance at low angles of attack. Conversely, a greater distance reduces the aerodynamic performance produced at high angles of attack (Fouatih *et al.* 2019). Similar to the statement from Fig. 12a-c, when the angle of attack is at a low angle of attack ($0° \leq \alpha \leq 10°$), among the other three variations, the 1.6 *h* VG provides the best performance, although at the angle of attack ($0° \leq \alpha \leq 8°$), the addition of the VG with the three variations studied does not give positive results. This happens because at the angle of attack ($0° \leq \alpha \leq 8°$), the vorticity generated by the three VGs is too large and produces unnecessary drag, as shown in Fig. 12b. The additional drag compensates for the C_L value in Fig. 12a, thus deteriorating the aerodynamic performance. Different results are encountered when the angle of attack is at ($12° \leq \alpha \leq 16°$). The 0.8 *h* VG provides the best performance, followed by the 1.2 *h* and 1.6 *h* variations, respectively. At a high angle of attack ($12° \leq \alpha \leq 16°$), only the 0.8 *h* variation can provide better performance compared to the benchmark performance, namely an increase in the *L/D* ratio of 3.52%–29.96%.

Figure 13 represents the turbulence intensity at the critical angle of attack. At that angle, the vane distance of 0.8 *h* can reduce the turbulence intensity that occurs before using the VG, which is the most effective variation compared to the other variations.

Effect of VG location from the leading edge

The VG location influences the aircraft's aerodynamic behavior and capacity. The optimal location for the placement of the VG changes as the angle of attack changes. To find the most optimal installation location of the VG, three height variations of the VG were simulated, namely 0.10 *L*, 0.125 *L*, and 0.15 *L*, while maintaining a VG height of 20 mm, a length of 3 *h*, an angle of incidence of 10°, and a distance between VGs of 1.2 *h* for each variation.

Figure 14a-c shows the position effect on the C_L, C_D, and performance efficiency at various angles. Figures 14a and b indicate that a mounting position closer to the separation point occurring at that angle provides a higher lift increase accompanied by a slight increase in drag. This is because the installation of the VG is too far from the upstream position, causing more and more areas to be affected by the VG (De Tavernier *et al.* 2021).

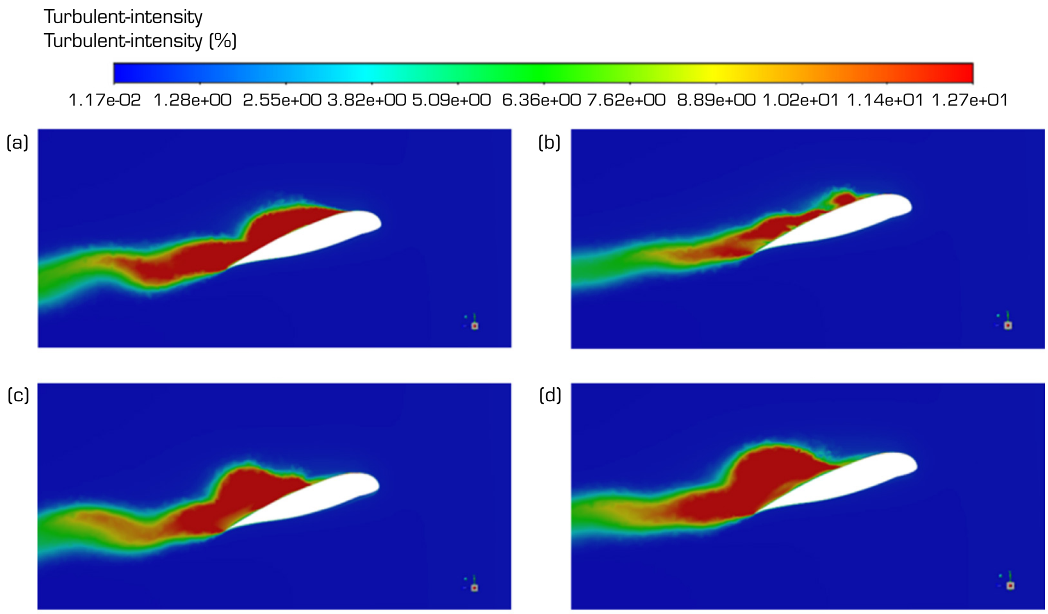

Source: Elaborated by the authors.

Figure 13. Contour of the effect of the distance between the vane on turbulence intensity. (a) Baseline; (b) 0.8 *h*; (c) 1.2 *h*; (d) 1.6 *h*.

Figure 14c shows that the presence of the VG at the angle of attack (α ≤ 14°) adversely impacts the aircraft's aerodynamic capability. This event is caused by the vortex flow generated by the VG ruining the flow of the boundary layer that interacts on the surface (Agarwal and Kumar 2016; De Tavernier *et al.* 2021). The increase in the best *L/D* ratio value when the angle of attack is at (α =16°) can be seen in the installation of the VG at the location of 0.125 *L*, which is 20.73%, and an increase in the *L/D* value of around 8.60% occurs in the installation of the VG at 0.10 *L* at (α = 18°). This result is reinforced by the statement of Fouatih *et al.* (2019), who stated that the upstream position of the VG decreases the *L/D* at the low angles of attack and increases it as the angle of attack increases. Figure 15 shows the intensity of turbulence that occurs at each variation at (α = 16°).

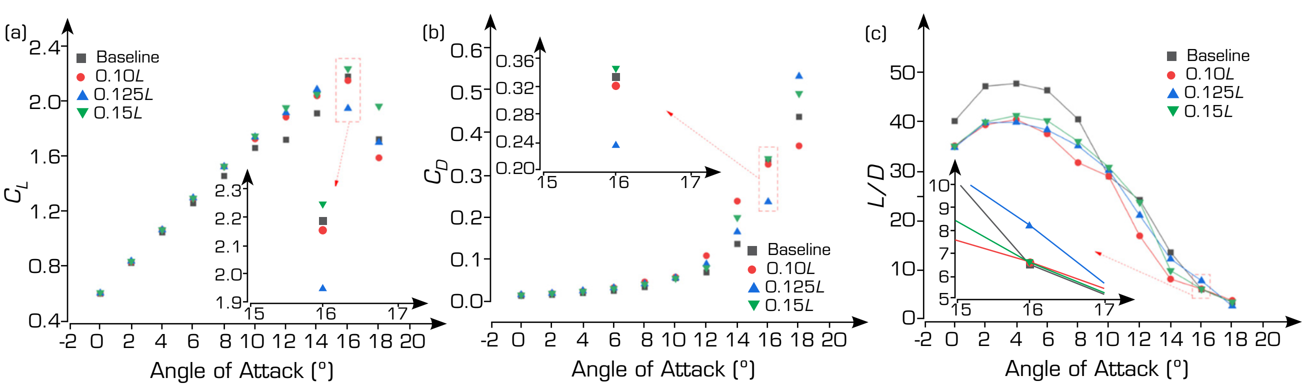

Source: Elaborated by the authors.

Figure 14. Effect of VG location from the leading edge on: (a) C_L; (b) C_D; (c) *L/D*.

Effect of vane angle of incidence

The angle of the installation of the VG relative to the direction of the wind flow rate affects the strength of the vortex flow produced. Three variations of the angle of incidence of the VG were simulated, namely 10°, 14°, and 18° by maintaining the position of the VGs at 0.15 *L*, a length of 20 mm, a height of 3 *h*, and a distance between vanes of 1.2 *h*.

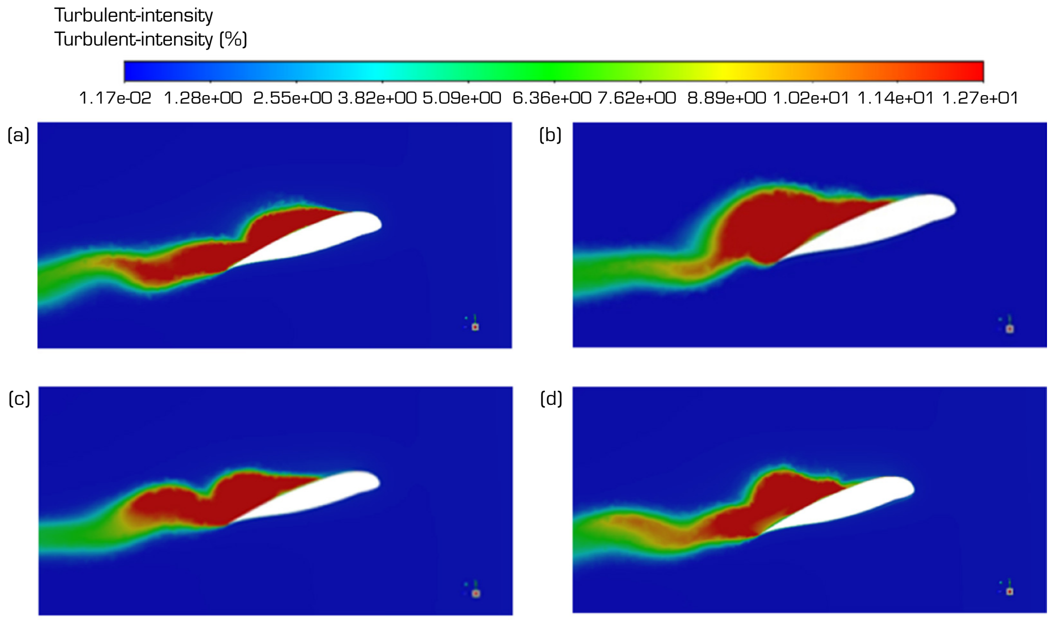

Source: Elaborated by the authors.

Figure 15. Contour of the effect of the VG location from the leading edge on turbulence intensity. (a) Baseline; (b) 0.10 *L*; (c) 0.125 *L*; (d) 0.15 *L*.

The angle of the VG installation relative to the direction of the wind flow rate affects the strength of the generated vortex flow. In general, the greater the angle difference between the angle of installation of the VG and the angle of arrival of the airflow, the greater the vortex force will be produced (Ibarra-Udaeta *et al.* 2019). The amount of vortex produced affects aerodynamic performance; if the vortex produced is too small, it is not be effective in improving the flow around the airfoil, whereas large vorticity increases the value of the C_D, which can have an impact on decreasing aerodynamic performance.

Figure 16a-c points out that the effective mounting angle varies with an increase in the angle of attack. Figure 16a shows that the mounting angle producing the highest C_L at the angle of attack ($0° \leq \alpha \leq 12°$) is found at the angle of incidence of 14°. In comparison, when the angle of attack is at ($12° \leq \alpha \leq 18°$), the angle of incidence of 16° produces the best C_L value. In addition, the VG with an 18° mounting angle successfully delays stall occurring at an angle of attack of 16° to at least 18°.

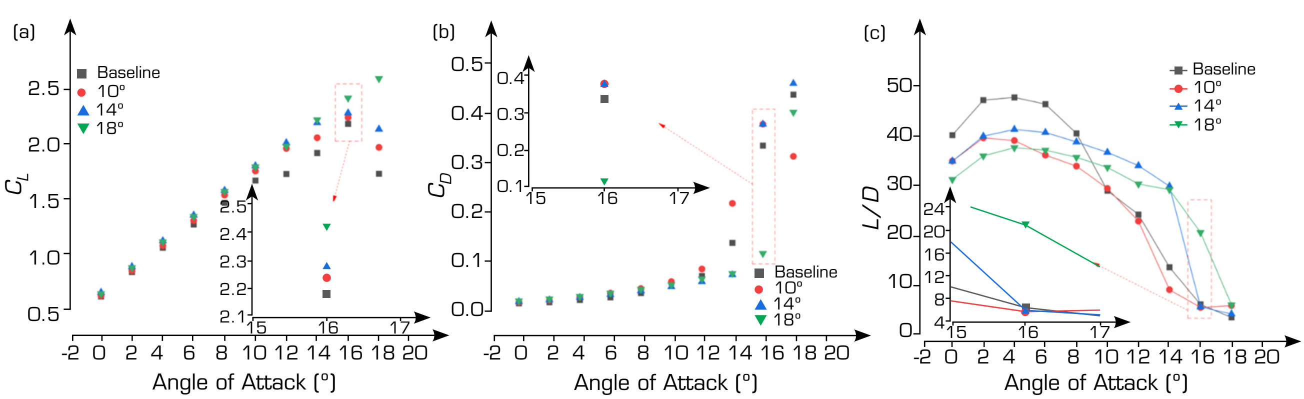

Source: Elaborated by the authors.

Figure 16. Effect of vane angle of incidence on: (a) C_L; (b) C_D; (c) *L/D*.

Based on Fig. 16c, it can be seen that the incidence angle of the VG affects the effectiveness of aerodynamic performance. The addition of a VG when at a low angle of attack (0° ≤ β ≤ 8°) has a harmful effect. At the angle of attack (10° ≤ α ≤ 14°), a 14° angle of approach gives an increase in *L/D* of 26.16%–115.80%, while an 18° angle of incidence results in an increase in *L/D* of 15.92%–110.83%. The 18º angle of approach successfully delays the separation so that it can increase the stall angle from 16°, where at (16° ≤ α ≤ 18°), the 18° angle of incidence results in an increase in *L/D* of up to 63.34%–219.21% from the initial performance. A VG with a high angle of incidence is effective at a high angle of attack, while a VG with a low angle of incidence is effective when the angle of attack is low (Fouatih *et al.* 2019).

Each variation in the mounting angle has a different effect on improving the airflow occurring around the wings, which can be seen from the intensity of the turbulence that occurs. Figure 17 illustrates the flow around the airfoil at the critical angle of attack, where the image contains a comparison of the turbulence intensity occurring before and after the installation of the VG at each variation of the installation angle. The 18° mounting angle can be seen to have a positive effect in controlling the flow around the VG, as shown by the absence of red high turbulence intensity around the airfoil.

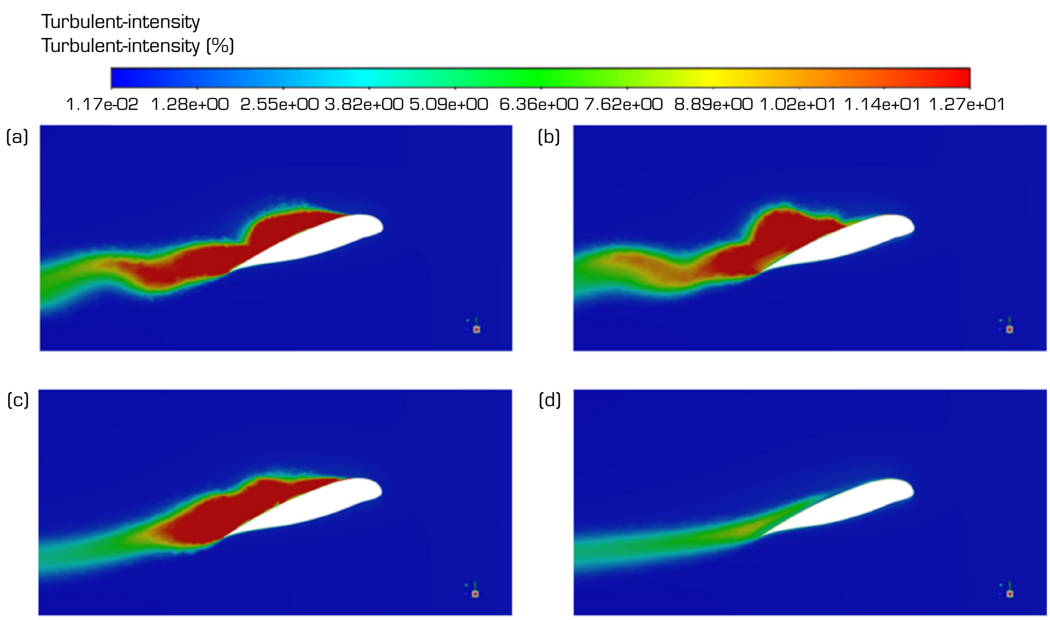

Source: Elaborated by the authors.

Figure 17. Contour of the effect of the vane angle of incidence on turbulence intensity.

CONCLUSION

The results of the study using the numerical simulation method can show that the geometric parameters and mounting position affect the amount of vortex force generated and influence the aerodynamic capabilities of the amphibious aircraft.

The following conclusions can be observed:

- Within the angle of attack (0° ≤ α ≤ 8°), the entire addition of the VG had a negative impact on the aerodynamic efficiency, as shown by the *L/D* ratio. In comparison, at a range of (10° ≤ α ≤ 16°), the variation of 30 mm showed the best result, which was to increase the *L/D* ratio by 20.42%–57.94% compared to the baseline performance.
- Within the angle of attack (0° ≤ α ≤ 8°), all the additions of the VGs had a negative impact on the *L/D* ratio, while at the angle of attack (8° ≤ α ≤ 16°), the 4.5 *h* variation showed the best result, namely increasing the *L/D* ratio by 0.15%–136.02% compared to the baseline performance.
- Within the angle of attack (0° ≤ α ≤ 8°), the addition of the VG had a negative impact on the *L/D* ratio. In comparison, at the angle of attack (α = 10°), the 1.6 *h* variation managed to provide an increase in the *L/D* ratio of 6.54%. In the angle of attack

(12° ≤ α ≤ 16°), the 0.8 *h* variation showed the best result, which was to increase the *L/D* ratio by 3.52%–29.96% compared to the baseline performance.

- Within the angle of attack (0° ≤ α ≤ 8°), the entire addition of the VG had a negative impact on the *L/D* ratio. At an angle (α = 10°), the variation of 0.125 *L* and 0.15 *L* succeeded in increasing the *L/D* ratio by 4.02% and 6.16%, respectively, while at the critical angle of attack, the 0.125 *L* mounting position provided the highest *L/D* increase of 26.15% compared to without using the VG.
- Within the angle of attack (0° ≤ α ≤ 8°), the entire addition of the VG has adversely affected the *L/D* ratio. At the angle of attack (10° ≤ α ≤ 14°), a 14° angle of incidence yielded an enhancement in *L/D* of 26.16%–115.80%, while an 18° angle of incidence produced an improvement in *L/D* of 15.92%–110.83%. The angle of incidence of 18° successfully delayed the separation so that it could increase the stall angle from 16°, where at the angle of attack (16° ≤ α ≤ 18°), the 18° angle of incidence lead to an increase in *L/D* of up to 63.34%–219.21% compared to without the use of the VG.

In summary, the configuration with h = 30 mm and l = 4.5 h provided the most significant improvement in aerodynamic efficiency at high angles of attack. While the implementation of counter-rotating VGs significantly enhances lift and delays stall at high angles of attack, it is essential to consider the associated drag penalty. At low angles of attack typical of cruise flight (0° ≤ α ≤ 8°), the VGs act as additional surface obstructions that increase parasitic drag, as evidenced in Fig. 7. Consequently, this technology is most economically feasible for short-haul amphibious operations where the cruise phase is relatively brief and the operational priority is safely accessing hard-to-reach airfields with short runways. For such specific missions, the gain in STOL performance and the increased safety margins during take-off and landing justify the marginal increase in fuel consumption and emissions during the short transit phase.

Ultimately, this study confirms that VGs are a viable passive flow control method for improving the operational safety of STOL amphibious aircraft.

CONFLICTS OF INTEREST

Nothing to declare.

AUTHOR CONTRIBUTIONS

Conceptualization: Wijiatmoko G; **Methodology:** Wijiatmoko G and Pane IZ; **Software:** Maulana BE; **Validation:** Maulana BE and Bahar S; **Formal analysis:** Yohana E and Tauviqirrahman M; **Writing - Original Draft:** Maulana BE and Bahar S; **Writing - Review & Editing:** Yohana E and Tauviqirrahman M; **Visualization:** Maulana BE; **Supervision:** Yohana E and Tauviqirrahman M; **Project administration:** Pane IZ; **Funding acquisition:** Wijiatmoko G; **Final approval:** Wijiatmoko G.

DATA AVAILABILITY STATEMENT

The data will be available upon request.

FUNDING

National Research and Innovation Agency
Grant No: 8/III.3/HK/2024

DECLARATION OF USE OF ARTIFICIAL INTELLIGENCE TOOLS

No research data was generated by artificial intelligence.

ACKNOWLEDGEMENTS

Not applicable.

REFERENCES

[ITTC] International Towing Tank Conference (2011) Practical guidelines for ship CFD applications. ITTC Recommended Procedures and Guidelines 1-18. [accessed May 28, 2026]. https://www.ittc.info/media/11958/75-03-02-03.pdf

Agarwal S, Kumar P (2016) Numerical investigation of flow field and effect of varying vortex generator location on wing performance. Am J Fluid Dyn 6:11-19. [accessed May 28, 2026]. https://www.semanticscholar.org/paper/Numerical-Investigation-of-Flow-Field-and-Effect-of-Agarwal-Kumar/7b58e8f7eb767d8233f6ee122afa12f4db6013f1

Algan M, Seyhan M, Sarioğlu M (2024) Effect of aero-shaped vortex generators on NACA 4415 airfoil. Ocean Eng 291. https://doi.org/10.1016/j.oceaneng.2023.116482

Aliffrananda MHN, Sulisetyono A, Hermawan YA, Zubaydi A (2022) Numerical analysis of floatplane porpoising instability in calm water during takeoff. Int J Technol 13:190-201. https://doi.org/10.14716/ijtech.v13i1.4903

Bao S, Hu X, Wang J, Ma T, Rao Y, Deng Z (2020) Numerical study on the influence of initial ambient temperature on the aerodynamic heating in the tube train system. Adv Aerodyn 2. https://doi.org/10.1186/s42774-020-00053-8

Chen H (2021) Numerical investigation of the effects of vortex generators on the Bell A821201 airfoil. J Braz Soc Mech Sci Eng 43. https://doi.org/10.1007/s40430-021-03239-3

Chung PH, Huang YX, Chung KM, Huang CY, Isaev S (2023) Effective distance for vortex generators in high subsonic flows. Aerospace 10. https://doi.org/10.3390/aerospace10040369

De Tavernier D, Ferreira C, Viré A, LeBlanc B, Bernardy S (2021) Controlling dynamic stall using vortex generators on a wind turbine airfoil. Renew Energy 172:1194-1211. https://doi.org/10.1016/j.renene.2021.03.019

Duan X, Sun W, Chen C, Wei M, Yang Y (2019) Numerical investigation of the porpoising motion of a seaplane planing on water with high speeds. Aerosp Sci Technol 84:980-994. https://doi.org/10.1016/j.ast.2018.11.037

Fouatih OM, Imine B, Medale M (2019) Numerical/experimental investigations on reducing drag penalty of passive vortex generators on a NACA 4415 airfoil. Wind Energy 22:1003-1017. https://doi.org/10.1002/we.2330

Fouatih OM, Medale M, Imine O, Imine B (2016) Design optimization of the aerodynamic passive flow control on NACA 4415 airfoil using vortex generators. Eur J Mech B Fluids 56:82-96. https://doi.org/10.1016/j.euromechflu.2015.11.006

Golmirzaee N, Wood DH (2024) Some effects of domain size and boundary conditions on the accuracy of airfoil simulations. Adv Aerodyn 6. https://doi.org/10.1186/s42774-023-00163-z

Große C, Olausson PM, Svensson B (2021) Resilience endangered: The role of regional airports in remote areas in Sweden. Infrastructures (Basel) 6. https://doi.org/10.3390/infrastructures6120167

Hafien C, Mbarek T Ben (2019) Reduced order model for the lift coefficient of an airfoil equipped with extrados and/or trailing edge flexible flaps. Comput Fluids 180:82-95. https://doi.org/10.1016/j.compfluid.2018.11.029

Hao L, Hu B, Gao Y, Wei B (2023) Effect of vortex generator spanwise height distribution pattern on aerodynamic characteristics of a straight wing. Adv Aerodyn 5. https://doi.org/10.1186/s42774-023-00137-1

Hares H, Mebarki G, Brioua M, Naoun M (2019) Aerodynamic performances improvement of NACA 4415 profile by passive flow control using vortex generators. J Serbian Soc Comput Mech 13:17-38. https://doi.org/10.24874/jsscm.2019.13.01.02

Ibarra-Udaeta I, Errasti I, Fernandez-Gamiz U, Zulueta E, Sancho J (2019) Computational characterization of a rectangular vortex generator on a flat plate for different vane heights and angles. Appl Sci (Switz) 9. https://doi.org/10.3390/app9050995

Ichikawa Y, Koike S, Ito Y, Murayama M, Nakakita K, Yamamoto K, Kusunose K (2021) Size effects of vane-type rectangular vortex generators installed on high-lift swept-back wing flap on lift force and flow fields. Exp Fluids 62. https://doi.org/10.1007/s00348-021-03198-4

Jiang H, Yao W, Xu M (2023) Experimental design for a novel co-flow jet airfoil. Adv Aerodyn 5. https://doi.org/10.1186/s42774-023-00161-1

Karyawan, Suwasono B, Sutiyo, Syamsuar S, Fajar R, Triputra FR. (2024) Hydrodynamic characteristics for catamaran floatplane in taxiing conditions. Int Rev Aerosp Eng 17:1-11. https://doi.org/10.15866/irease.v17i1.24489

Khaled MF, Aly AM (2022) Assessing aerodynamic loads on low-rise buildings considering Reynolds number and turbulence effects: a review. Adv Aerodyn 4. https://doi.org/10.1186/s42774-022-00114-0

Li T, Liang H, Xiang Z, Zhang J (2024) Numerical study on the effect of vortex generators on the aerodynamic drag of a high-speed train. Fluid Dyn Mater Process 20:463-473. https://doi.org/10.32604/fdmp.2023.043618

Li T, Liang H, Zhang J, Zhang J (2023) Numerical study on aerodynamic resistance reduction of high-speed train using vortex generator. Eng Appl Comput Fluid Mech 17. https://doi.org/10.1080/19942060.2022.2153925

Li X, Yang K, Wang X (2019) Experimental and numerical analysis of the effect of vortex generator height on vortex characteristics and airfoil aerodynamic performance. Energies (Basel) 12. https://doi.org/10.3390/en12050959

Li XK, Liu W, Zhang TJ, Wang PM, Wang XD (2019) Analysis of the effect of vortex generator spacing on boundary layer flow separation control. Appl Sci (Switz) 9. https://doi.org/10.3390/app9245495

Manolesos M, Chng L, Kaufmann N, Ouro P, Ntouras D, Papadakis G (2023) Using vortex generators for flow separation control on tidal turbine profiles and blades. Renew Energy 205:1025-1039. https://doi.org/10.1016/j.renene.2023.02.009

Mazzola F, Cirà A, Ruggieri G, Butler R (2022) Air transport and tourism flows to islands: A panel analysis for southern European countries. Int J Tour Res 24:639-652. https://doi.org/10.1002/jtr.2527

Meyer J, Okfen P, Bil C (2021) Optimisation of vortex generators for stall speed reduction (doctoral dissertation). Boulder: University of Colorado at Boulder. [accessed May 28 2026]. https://www.icas.org/icas_archive/ICAS2020/data/papers/ICAS2020_0311_paper.pdf

Nath DS, Pujari PC, Jain A, Rastogi V (2021) Drag reduction by application of aerodynamic devices in a race car. Adv Aerodyn 3. https://doi.org/10.1186/s42774-020-00054-7

Radha Krishnan P, Mukesh R, Hasan I, Booma Devi P, Alebachew WA (2023) Comparative study and aerodynamic analysis of rectangular wing using high-lift systems. Int J Aerosp Eng 2023. https://doi.org/10.1155/2023/5813557

Rokhman F, Yohana E, Tauviqirrahman M, Faried MI, Yulianto ME, Choi HU, Lee DH (2024) Performance enhancement of falling film dehumidifier by variation number and width ratio rectangular cylinder based on CFD simulation. Int J Heat Mass Transf 221. https://doi.org/10.1016/j.ijheatmasstransfer.2023.125002

Seth A, Liem RP (2021) Amphibious aircraft developments: Computational studies of hydrofoil design for improvements in water-takeoffs. Aerospace 8:1-31. https://doi.org/10.3390/aerospace8010010

Sulistiya S, Kasman AS (2019) Validasi model turbulensi pada simulasi numerik menggunakan software Fluent dengan sayap Onera M6. J Aero Technol 2. https://doi.org/10.29122/joat.v2i1.3817

Szabó A, Nagy PT, De Baets G, Vanierschot M, Paál G (2024) Stability analysis of a streaky boundary layer generated by miniature vortex generators. Comput Fluids 269. https://doi.org/10.1016/j.compfluid.2023.106123

Tleubergenova AZ, Tanasheva NK, Shaimerdenova KM, Kassymov SS, Bakhtybekova AR, Shuyushbayeva NN, Uzbergenova SZ, Ranova GA (2023) Mathematical modeling of the aerodynamic coefficients of a sail blade. Adv Aerodyn 5. https://doi.org/10.1186/s42774-023-00140-6

Tsipenko VG, Sagaydak MV, Shevyakov VI (2022) The use of vortex generators to improve the take-off and landing characteristics of transport category aircraft. Civ Aviat High Technol 25:83-95. https://doi.org/10.26467/2079-0619-2022-25-4-83-95

Utomo MSKTS, Yohana E, Mahendra C, Utama IY (2024) Analysis of blended winglet parameters on the aerodynamic characteristics of NXXX aircraft using Computational Fluid Dynamics (CFD). Results Eng 24. https://doi.org/10.1016/j.rineng.2024.102901

van Druenen T, Blocken B (2023) Aerodynamic impact of cycling postures on drafting in single paceline configurations. Comput Fluids 257. https://doi.org/10.1016/j.compfluid.2023.105863

Verma S, Sankar M (2024) Improved effectiveness of vane-type vortex generators for incident shock-induced separation. AIAA J 2024:1-17. https://doi.org/10.2514/1.J064000

Wang X, Hu X, Wang P, Zheng J, Li H, Deng Z, Zhang W (2023) Numerical simulation and optimization on opening angles of aerodynamic braking plates sets for a maglev train. Adv Aerodyn 5. https://doi.org/10.1186/s42774-023-00144-2

Wijiatmoko G, Yohana E, Adi Nugroho P, Tauviqirrahman M, Zuhdi Pane I (2024) CFD analysis of counter-rotating vane-type wing vortex generator for regional aircraft. CFD Lett 16:1-16. https://doi.org/10.37934/cfdl.16.11.116

Yan Y, Avital E, Williams J, Cui J (2019) CFD analysis for the performance of micro-vortex generator on aerofoil and vertical axis turbine. J Renew Sustain Energy 11. https://doi.org/10.1063/1.5110422

Zhen TK, Zubair M, Ahmad KA (2011) Experimental and numerical investigation of the effects of passive vortex generators on Aludra UAV performance. Chin J Aeronaut 24:577-583. https://doi.org/10.1016/S1000-9361(11)60067-8

Zhu C, Chen J, Qiu Y, Wang T (2021) Numerical investigation into rotational augmentation with passive vortex generators on the NREL Phase VI blade. Energy 223. https://doi.org/10.1016/j.energy.2021.120089